

Original article

The quantitative assessment of interstitial lung disease with positron emission tomography scanning in systemic sclerosis patients

Daphne M. Peelen¹, Ben G. J. C. Zwezerijnen², Esther J. Nossent³, Lilian J. Meijboom², Otto S. Hoekstra², Conny J. Van der Laken¹ and Alexandre E. Voskuyl¹

Abstract

Objectives. The reversibility of interstitial lung disease (ILD) in SSc is difficult to assess by current diagnostic modalities and there is clinical need for imaging techniques that allow for treatment stratification and monitoring. ¹⁸F-Fluorodeoxyglucose (FDG) PET/CT scanning may be of interest for this purpose by detection of metabolic activity in lung tissue. This study aimed to investigate the potential role of ¹⁸F-FDG PET/CT scanning for the quantitative assessment of SSc-related active ILD.

Methods. ¹⁸F-FDG PET/CT scans and high resolution CT scans of eight SSc patients, including five with ILD, were analysed. For comparison, reference groups were included: eight SLE patients and four primary Sjögren's syndrome (pSS) patients, all without ILD. A total of 22 regions of interest were drawn in each patient at apical, medial and dorsobasal lung levels. ¹⁸F-FDG uptake was measured as mean standardized uptake value (SUVmean) in each region of interest. Subsequently, basal/apical (B/A) and medial/apical (M/A) ratios were calculated at patient level (B/A-p and M/A-p) and at tissue level (B/A-t and M/A-t).

Results. SUVmean values in dorsobasal ROIs and B/A-p ratios were increased in SSc with ILD compared with SSc without ILD ($P=0.04$ and $P=0.07$, respectively), SLE ($P=0.003$ and $P=0.002$, respectively) and pSS ($P=0.03$ and $P=0.02$, respectively). Increased uptake in the dorsobasal lungs and increased B/A-t ratios corresponded to both ground glass and reticulation on high resolution CT.

Conclusion. Semi-quantitative assessment of ¹⁸F-FDG PET/CT is able to distinguish ILD from non-affected lung tissue in SSc, suggesting that it may be used as a new biomarker for SSc-ILD disease activity.

Key words: Systemic sclerosis, interstitial lung disease, lung fibrosis, ¹⁸F-FDG PET/CT, positron emission tomography

Rheumatology key messages

- Semi-quantitative assessment of ¹⁸F-FDG PET/CT distinguishes ILD from healthy lung tissue.
- Increased ¹⁸F-FDG uptake in SSc-ILD lungs corresponds to ground glass and reticulation on high resolution CT.
- Semi-quantitative ¹⁸F-FDG PET/CT analysis could potentially be used as a biomarker for assessing SSc-ILD disease activity.

Introduction

Interstitial lung disease (ILD) is the main cause of death in SSc patients [1]. Up to 90% of SSc patients will develop

some degree of ILD, of which 30% have severe disease resulting in increased morbidity and mortality [2–4]. Available treatment options for SSc-ILD have limited effect and are potentially associated with severe drug side effects, making the management of SSc-ILD a challenge in clinical practice [5, 6].

Currently, to determine whether treatment should be initiated and for evaluation of treatment response, pulmonary functions tests (PFT) and high resolution CT (HRCT) are used as the most important tools. The pattern of ILD can be assessed with HRCT. In SSc-ILD patients, most commonly a radiological pattern of non-specific

¹Department of Rheumatology, Amsterdam Rheumatology & Immunology Center, ²Department of Radiology and Nuclear Medicine and ³Department of Pulmonary Medicine and Amsterdam Cardiovascular Sciences, Amsterdam UMC, Vrije Universiteit, Amsterdam, The Netherlands

Submitted 19 April 2019; accepted 25 August 2019

Correspondence to: Alexandre E. Voskuyl, Department of Rheumatology, VU University Medical Center, PO Box 7057, 1007 MB Amsterdam, The Netherlands. E-mail: ae.voskuyl@vumc.nl

interstitial pneumonia (NSIP) is seen, and less often a usual interstitial pneumonia or other ILD pattern [2]. Decrease of lung function can be assessed with PFT, in which the forced vital capacity and the diffusion capacity for carbon monoxide are the most indicative parameters of disease progression [7]. However, there is a need for other tools and biomarkers, as HRCT provides morphological rather than functional information and therefore is only indirectly related to disease activity [4, 5, 8–10]. Novel approaches to directly assess disease activity and to monitor the efficacy of drug treatment are therefore needed.

Recently, the use of ^{18}F -fluorodeoxyglucose (FDG) PET/CT scanning for the assessment of ILD has been investigated [11–16]. It has been shown that ^{18}F -FDG PET/CT scanning is a non-invasive and sensitive method to detect inflammation as a result of increased glucose metabolism in inflammatory cells; activated neutrophils, lymphocytes and macrophages, known to be involved in SSc-ILD pathogenesis, highly express GLUT1 and GLUT3 receptors through which ^{18}F -FDG cell uptake is facilitated [11, 17–19]. Also, fibrotic cells in lungs with ILD may show increased cell metabolism [19]. Histopathological studies showed an accumulation of inflammatory cells in HRCT-classified fibrotic lesions as well [12, 17, 20, 21]. Therefore, differentiation of active and inactive disease based on the detection of inflammation or fibrosis on HRCT seems to be inaccurate. Combining functional ^{18}F -FDG PET/CT information with anatomical HRCT information could potentially improve the understanding of underlying processes or the evaluation of disease activity in SSc-ILD patients.

Previous studies have shown that semi-quantitative ^{18}F -FDG PET/CT scan analysis might be useful to assess disease activity in patients with SSc-ILD and related conditions [12–16, 22–29]. However, ^{18}F -FDG PET/CT studies with SSc-ILD patients thus far have limitations in regard to quantification [12, 23, 24, 29]. The challenge of quantification is emphasized by the fact that the NSIP pattern is characterized by local variability in the amount of cellular infiltrates and fibrotic areas [30, 31]. ^{18}F -FDG PET/CT analysis that accounts for this localized disease activity is therefore important. Furthermore, variations of air and perfusion in the lungs are known to strongly influence the measured ^{18}F -FDG uptake [32, 33]. Therefore it is important to take into account that physiological craniocaudal gradients of perfusion and ventilation may lead to false-positive or -negative ^{18}F -FDG signals [34, 35]. Another essential step in quantification is the correction for inter-individual variability in ^{18}F -FDG metabolism, which can be obtained by correcting standardized uptake values (SUVs) with the level of ^{18}F -FDG uptake in the mediastinal blood pool [27]. These facts highlight the need for the development of a new quantitative ^{18}F -FDG PET/CT analysis method for SSc-ILD that accounts for localized disease activity, craniocaudal gradients and inter-individual variability.

The aim of this study was to investigate the potential value of semi-quantitative ^{18}F -FDG PET/CT scan analysis for the assessment of ILD in SSc patients. For this

purpose, we developed a new method for semi-quantitative ^{18}F -FDG PET/CT analysis. We used this method to retrospectively analyse ^{18}F -FDG PET/CT scans of SSc patients with and without ILD and disease control groups. Subsequently, we related those findings to those of the HRCT scans.

Methods

Study design and patients

This retrospective study was performed in the Amsterdam UMC, Vrije Universiteit Amsterdam, The Netherlands. In-hospital databases were searched for ^{18}F -FDG PET/CT scans of SSc patients that were performed between 2007 and 2017. Eight SSc patients were diagnosed according to the ACR/ EULAR classification criteria for SSc [36]. Five out of eight SSc patients were diagnosed with ILD [3, 30]. As disease controls, SLE patients and pSS patients who met the 1997 ACR criteria and the 2016 ACR/EULAR classification criteria for SLE and pSS, respectively, were included [37, 38]. None of the control patients was diagnosed with ILD. Exclusion criteria were: patients with overlap between SSc, SLE or pSS, and patients with lung cancer or metastasis, pulmonary sarcoidosis, infectious pneumonia and shrinking lung syndrome. This study was exempt from approval of an ethics committee due to the retrospective character. ^{18}F -FDG PET/CT scans were performed as part of clinical care with several indications: (suspicion of) malignancy ($n = 13$), suspicion of infection/abscess ($n = 6$) and suspicion of relapse aortitis ($n = 1$).

^{18}F -FDG PET/CT protocol

^{18}F -FDG PET/CT scans were performed according to the European Association of Nuclear Medicine procedure guidelines [39]. Patients were instructed to fast for 6 h prior to scanning. Mean serum glucose level was 5.5 mmol/l (range 5.2–6.1 mmol/l). ^{18}F -FDG PET/CT acquisition (skull vertex to mid-thigh) was acquired ~60 min after intravenous administration of 147–275 MBq ^{18}F -FDG, depending on body weight. The ^{18}F -FDG PET/CT scans (4 min per bed position, 512 × 512 matrix, axial field view of 18 cm) were performed with the Philips Gemini TF-64 PET-CT scanner (Philips Medical Systems, Best, The Netherlands). Low-dose CT was performed with 120 kV and 30 mAs prior to emission scanning.

^{18}F -FDG PET/CT analysis

Philips IntelliSpace Portal software was used for ^{18}F -FDG PET/CT analysis. Visual examination of ^{18}F -FDG PET/CT scans for the detection of increased ^{18}F -FDG uptake in lungs was performed by scrolling up and down through sagittal, coronal and transverse whole-body slides of each patient. This visual examination was performed by a nuclear medicine physician who was blinded for the diagnosis of ILD, but not for the diagnosis of SSc, SLE and pSS.

To semi-quantitatively assess the ^{18}F -FDG uptake in lungs, we developed a multi-level analysis protocol that is feasible for the detection of localized disease activity, as

followed: in each patient, a total of 22 regions of interest (ROIs) of diameter size 2 cm were drawn at apical, medial and basal lung levels. The apical and medial levels were estimated in transverse slides in plane with the upper wall of the aortic arch and just below the carina, respectively. To avoid measuring ^{18}F -FDG uptake in the basal lung field projected from the liver (by spill-over and diaphragmatic motion-related artifacts), ROIs in the basal lung field were drawn 2.5 cm cranially from the posterocaudal lung borders (Supplementary Fig. S1, available at *Rheumatology* online). Subsequently, in transverse slides three posterior ROIs were drawn for each level in both lungs. Also, a ventral ROI was drawn at apical and medial levels. The mean SUVmean (the mean of SUVmean) was measured in all 22 ROIs. SUVmean of the mediastinal blood pool (MBP) was measured central-intraluminally in the aorta descendens at medial ROI level. SUVmean values of all ROIs were divided by the MBP in order to correct for inter-individual variability. All ROI drawings and SUVmean measurements were performed twice by one trained researcher and repeated once by a nuclear medicine physician. Both were blinded for the diagnosis of autoimmune disease and for the diagnosis of ILD. The second researcher was also blinded for the SUV measurements of the first researcher.

HRCT protocol

HRCT scans were conducted using a multidetector row spiral CT scanner (Sensation 64, Siemens Medical System, Forchheim, Germany; Discovery CT750HD, GE Medical System, Waukesha, WI, USA; or iCT256, Philips Medical System, Cleveland, OH, USA) with 64 or 256 detector arrays. Patients were scanned in supine position during one breath hold at a deep inspiration. Target thin-section helical CT scans of 1.0 or 1.25 mm collimation were obtained and reconstructed using a high-spatial-frequency algorithm.

HRCT analysis

In each SSc-ILD patient, the HRCT scan was performed within 3 months before or after the ^{18}F -FDG PET/CT scans. In SSc patients without ILD, HRCT scans were performed within 4 months before or after ^{18}F -FDG PET/CT scans.

HRCT scans were re-assessed by an experienced radiologist and pulmonologist specialized in ILD, blinded for the clinical data of the patients. Radiological ILD patterns were defined according to the 2013 American Thoracic Society/ERS criteria and 2008 Goh criteria [3, 30]. In cases of ILD, specific radiological abnormalities were assessed in 22 ROI areas: normal lung parenchyma, ground glass, consolidation, reticulation, reticulation with architectural distortion or honeycombing. The HRCT ROI areas corresponded to the 22 ^{18}F -FDG PET/CT ROIs areas, as they were drawn at the same anatomical locations (Supplementary Fig. S1, available at *Rheumatology* online) [40]. All dorsobasal ROIs of the five SSc-ILD patients (total of 30 ROIs) were pooled for further analysis.

Basal/apical and medial/apical ratios

SUVmean ratios were calculated to investigate if there are craniocaudal gradients of ^{18}F -FDG uptake in ILD affected and healthy lungs. We calculated basal/apical (B/A) and medial/apical (M/A) ratios for this purpose. At patient level, the basal/apical ratio (B/A-p) was calculated as the average of six posterior basal SUVmean values (MBP corrected) divided by the average of six posterior apical SUVmean values (MBP corrected). Also, medial/apical ratios (M/A-p) were calculated with this formula, using the average of six posterior medial SUVmean values.

At tissue level, basal/apical and medial/apical ratios (B/A-t and M/A-t) were calculated according to the HRCT pattern: SUVmean values of each individual basal or medial ROI was divided by the average of six apical SUVmean values (MBP corrected). These individual ratios were grouped based on the HRCT score (1–6) and a mean ratio for each HRCT pattern group was calculated.

Statistical analysis

All statistical analyses were performed using GraphPad Prism Version 7.0c for Mac (GraphPad Software Inc., La Jolla, CA, USA). Normality was determined with the D'Agostino–Pearson normality test. Subsequently, an unpaired two-tailed *t*-test, Mann–Whitney *U* test or Kruskal–Wallis test was performed to compare groups. *P*-values <0.05 were considered to be statistically significant.

Results

Patient characteristics

The mean age of SSc patients with and without ILD was comparable, but pSS and SLE patients were significantly younger ($P=0.016$, Kruskal–Wallis test). Disease duration in SLE patients was higher compared with other groups, although not statistically significantly. An immunosuppressive drug at inclusion was used by one SSc-ILD patient (prednisone 5 mg per day), but not by any of the SSc without ILD patients. Seven out of eight SLE patients used one or more immunosuppressive drugs, varying among HCQ, prednisone and azathioprine. One pSS patient used prednisone and one pSS patient used HCQ at inclusion. All SSc-ILD patients had a NSIP pattern with >20% involvement of the lung parenchyma on HRCT (Table 1).

Visual examination of ^{18}F -FDG PET/CT scans

Upon first visual examination, ^{18}F -FDG PET/CT scans revealed higher ^{18}F -FDG uptake in dorsobasal lung fields of all SSc patients with ILD. No increased ^{18}F -FDG uptake in the lungs was seen in SSc without ILD, SLE and pSS patients (Fig. 1).

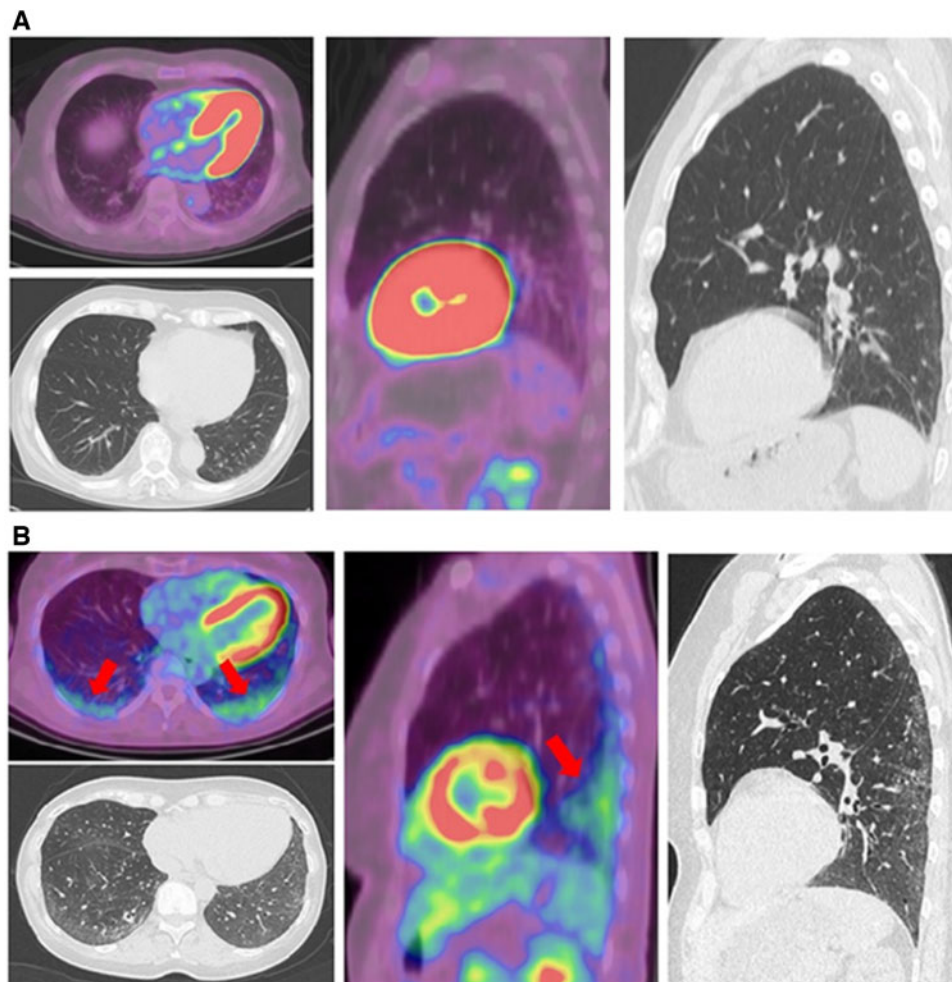
Semi-quantitative analysis of ^{18}F -FDG PET/CT scans

Significantly higher SUVmean values were found in dorsobasal ROIs of SSc patients with ILD compared with SSc patients without ILD, SLE patients and pSS patients ($P=0.04$, $P=0.003$ and $P=0.03$, respectively; Fig. 2). In

TABLE 1 Patient characteristics

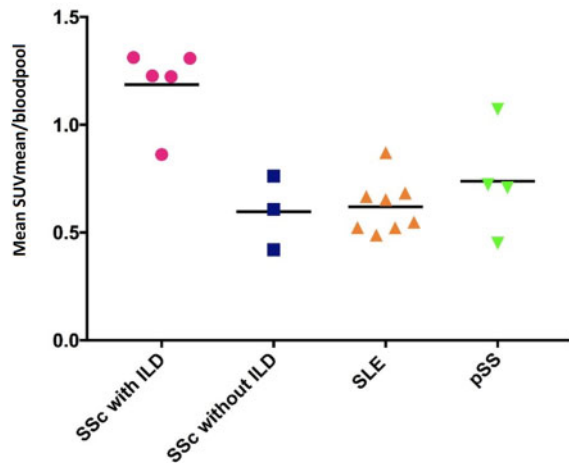
Characteristic	SSc patients with ILD (<i>n</i> = 5)	SSc patients without ILD (<i>n</i> = 3)	SLE patients (<i>n</i> = 8)	pSS patients (<i>n</i> = 4)
Age, mean, years	69.4	66.7	41.4	49.3
Female: male	4: 1	2: 1	7: 1	3: 1
Disease duration, mean, years	5.0	4.9	9.0	5.1
Current smoker, <i>n</i>	1	0	0	0
IS drugs, <i>n</i>	1	0	7	2
Limited SSc, <i>n</i>	3	2	—	—
Diffuse SSc, <i>n</i>	2	1	—	—
NSIP: UIP, <i>n</i>	5: 0	—	—	—
<20%, <i>n</i>	0	—	—	—
>20%, <i>n</i>	5	—	—	—

ILD: interstitial lung disease; IS: Immunosuppressive; NSIP: non-specific interstitial pneumonia; UIP: usual interstitial pneumonia.

FIG. 1 Visual examination of ^{18}F -FDG-PET and HRCT

Transverse and sagittal slides of ^{18}F -FDG-PET scans and HRCT scans of a SSc patient without ILD (**A**) and a SSc patient with ILD (**B**). Increased ^{18}F -FDG uptake in dorsobasal lung areas is marked by red arrows. FDG: fluorodeoxyglucose; HRCT: high resolution CT; ILD: interstitial lung disease.

Fig. 2 ^{18}F -FDG uptake in dorsobasal ROIs



Each data point represents the mean of six dorsobasal SUVmean values of a patient. Mean values for the different groups were: SSc with ILD: 1.19; SSc without ILD: 0.60; SLE: 0.62; pSS: 0.74. SUVmean values were significantly higher in the SSc with ILD group compared with the SSc without ILD patients, SLE patients and pSS patients ($P=0.04$, $P=0.003$ and $P=0.03$, respectively). Statistic test: Mann-Whitney U -test. FDG: fluorodeoxyglucose; ILD: interstitial lung disease; SUV: standardized uptake value; ROI: region of interest; SUVmean: mean SUV.

each SSc-ILD patient, the variation of SUVmean values between the six different dorsobasal ROI locations was low (Supplementary Fig. S2, available at *Rheumatology* online). Similar findings of low variation were found in the other patient groups (data not shown). Apical and medial SUVmean values in dorsal and ventral lung areas were low in all patient groups: mean SUVmean values were 0.45 in dorsoapical lung ROIs, 0.52 in dorsomedial lung ROIs, 0.40 in ventral apical lung ROIs and 0.40 in ventral medial ROIs (data not shown). B/A-p ratios were higher in SSc-ILD patients compared with SSc patients without ILD, SLE patients and pSS patients ($P=0.07$, $P=0.002$ and $P=0.02$, respectively; Fig. 3A). Mean B/A-p ratio of all control patients ($n=15$) was 1.43 (physiological craniocaudal ^{18}F -FDG gradient) and the B/A-p ratio of SSc-ILD patients ($n=5$) was 2.63 (pathological craniocaudal ^{18}F -FDG gradient). M/A-p ratios were comparable between the different patient groups; mean levels were: 1.23 in SSc-ILD patients, 1.18 in SSc without ILD patients, 1.10 in SLE patients and 1.12 in pSS patients (data not shown).

^{18}F -FDG-uptake in HRCT abnormalities

From a total of 30 dorsobasal ROIs of the five SSc-ILD patients, HRCT abnormalities were present in 38% of apical ROIs, 74% of medial ROIs and 96% of dorsobasal ROIs (Table 2). Honeycombing was not detected in the ROIs. Increased ^{18}F -FDG uptake was found in dorsobasal

ROIs that showed ground or reticulation. No increased or decreased ^{18}F -FDG uptake was measured in apical and medial HRCT abnormalities in comparison to normal lung parenchyma (Table 3). Compared with normal tissue, significantly higher B/A-t ratios were seen in areas of ground glass and in areas of reticulation with architectural distortion ($P=0.02$ and $P=0.02$, respectively; Fig. 3B). Mean levels of M/A-t ratios were 1.12 in normal radiological lung parenchyma, 1.52 in areas of ground glass, 1.32 in consolidation and 1.08 in reticulation (data not shown).

Discussion

In this study, we propose a newly developed semi-quantitative method of analysis for assessing ILD in SSc patients by using ^{18}F -FDG PET/CT. With this method, we were able to distinguish SSc-ILD patients from SSc, SLE and pSS patients without ILD, as we detected significantly increased ^{18}F -FDG uptake in dorsobasal lung fields in all SSc-ILD patients with a NSIP pattern compared and none in the control patients. This increased ^{18}F -FDG uptake was seen in areas with ground glass and reticulation, suggesting metabolic activity.

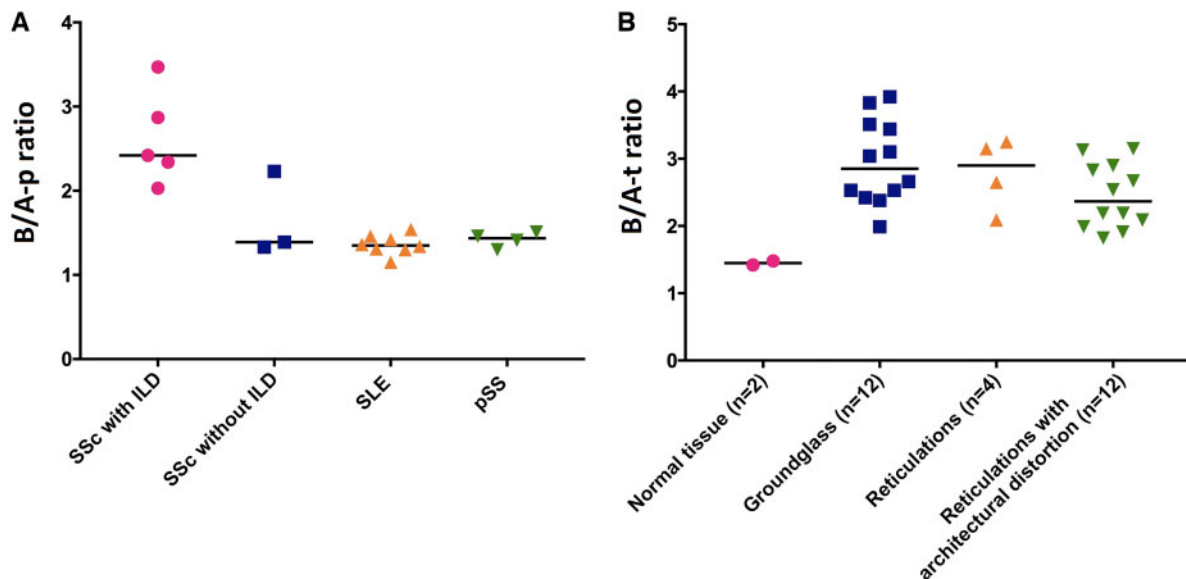
This study introduces a semi-quantitative method of analysis that included multi-level ROI analysis, mediastinal blood pool correction and a craniocaudal gradient calculation (ratios). With this approach we corrected for regional variations in disease activity, inter-individual variability and physiological craniocaudal gradients. This new method was tested in SSc patients with and without ILD and in two disease control groups as well. Quantification tools for ^{18}F -FDG PET/CT analysis in ILD patients were used in previous studies, but none of these studies combined all the quantification aspects and corrections as listed above [12, 13, 15, 16, 23, 26, 29].

With our multi-level ROI analysis, we showed that ^{18}F -FDG uptake in ILD-affected lungs varies in intensity and extent through the different lung areas of a patient. Thus, evaluating ILD disease activity with one single SUV value could lead to under- or overestimation. This multi-level approach is therefore preferable when assessing ILD disease activity with ^{18}F -FDG PET/CT scanning.

Our MBP correction reduced inter-individual variability, as ^{18}F -FDG levels in the blood pool including the pulmonary vascular bed vary among patients [41]. The MBP as background correction is already known as part of the Deauville scale for visual scoring of ^{18}F -FDG PET/CT scans [42]. We showed that the MBP is also feasible for semi-quantitative correction, by dividing raw SUVmean values by the MBP. The significance of this correction is strengthened by the fact that we found significant differences in SUV levels between MBP-corrected and -uncorrected data in our patients (data not shown).

Craniocaudal gradients of ventilation and perfusion are present in healthy lungs [34, 35]. Accounting for these physiological ventilation/perfusion gradients is important as it is known that air in the lungs reduces the ^{18}F -FDG signal as there is no ^{18}F -FDG uptake in air, whereas an increase in blood flow raises the ^{18}F -FDG signal [33]. We are the first to show that a physiological craniocaudal

Fig. 3 B/A-p and B/A-t ratios



(A) Mean values of B/A-p ratios were: SSc with ILD: 2.63; SSc without ILD: 1.65; SLE: 1.36; pSS: 1.42. The B/A-p ratio was higher in patients with ILD compared with patients without ILD, SLE patients and pSS patients ($P=0.07$, $P=0.002$ and $P=0.02$, respectively). (B) Mean values of B/A-t ratios were: normal lung parenchyma: 1.45; ground glass: 2.95; reticulation: 2.79; reticulation with architectural distortion: 2.45. The B/A-t ratio was significantly higher in areas of ground glass and in areas of reticulation with architectural distortion compared with normal lung parenchyma ($P=0.02$ and $P=0.02$, respectively), but not in areas of reticulation without architectural distortion ($P=0.13$). Statistic test: Mann-Whitney U -test. B/A-p ratio: basal/apical ratio at patient level; B/A-t ratio: basal/apical ratio at tissue level; ILD: interstitial lung disease; SUVmean: mean SUV.

TABLE 2 Radiological abnormalities on HRCT in SSc-ILD patients

Abnormality	Apical, n (%)	Medial, n (%)	Basal, n (%)
Normal lung parenchyma	17 (57)	8 (27)	2 (7)
Ground glass	5 (17)	8 (27)	12 (40)
Consolidation	4 (13)	1 (3)	0 (0)
Reticulation	4 (13)	13 (43)	4 (13)
Reticulation with architectural distortion	0 (0)	0 (0)	12 (40)

Pooled analysis of a total of 30 dorsobasal ROIs of five SSc-ILD patients. HRCT: high resolution CT; ILD: interstitial lung disease; ROI: region of interest.

^{18}F -FDG gradient is present in normal lungs as the B/A-p and M/A-p ratios were above 1 in all control patients. Therefore, accounting for this physiological gradient is in our opinion an essential step for a correct interpretation of disease activity with ^{18}F -FDG PET/CT scans. Moreover, higher B/A-p and M/A-p ratios were found in SSc-ILD patients showing that there is also a pathological craniocaudal gradient of ^{18}F -FDG uptake in SSc-ILD lungs. This is a

logical finding considering that the NSIP pattern is characterized by bilateral ground glass opacity and in most cases reticular opacities with traction bronchiectasis and bronchiolectasis [30, 31]. Therefore, the finding of an increased craniocaudal ^{18}F -FDG distribution gradient supports the idea that these areas are metabolically active.

In our study, markedly increased ^{18}F -FDG uptake was found in SSc-ILD lungs compared with normal lung tissue, whereas this increased uptake corresponded to areas with ground glass and reticulation on HRCT. Our results are in line with previous studies that also found increased ^{18}F -FDG uptake in ground glass and reticulation in patients with CTD-related ILD and idiopathic pulmonary fibrosis patients [12, 16, 23, 26, 29]. Several explanations for the increased ^{18}F -FDG uptake in ground glass and reticular lesions can be hypothesized. The development of lung fibrosis is an active process in which inflammation induces the fibrotic process of excessive extracellular matrix deposition. Many cell types are involved in this process, of which alternatively activated macrophages and activated fibroblasts play a key role in the course of inflammation and fibrosis, respectively [19, 43]. Both inflammation and fibrosis are characterized by increased cell metabolism and can therefore both explain the increased ^{18}F -FDG signal in SSc-ILD lungs [17, 19, 44]. Fibrotic areas may, however, also be non-active as well.

TABLE 3 ^{18}F -FDG uptake in different radiological abnormalities on HRCT

	Apical, mean SUVmean (range)	Medial, mean SUVmean (range)	Basal, mean SUVmean (range)
Normal lung parenchyma	0.39 (0.26–0.49)	0.45 (0.32–0.57)	0.53 (0.52–0.54)
Ground glass	0.55 (0.50–0.65)	0.68 (0.59–0.78)	1.27 (1.01–1.48)
Consolidation	0.63 (0.57–0.70)	0.80 (0.80–0.80)	
Reticulation	0.53 (0.45–0.67)	0.52 (0.42–0.79)	1.03 (0.77–1.20)
Reticulation with architectural distortion			1.27 (1.10–1.44)

FDG: fluorodeoxyglucose; HRCT: high resolution CT; Mean SUVmean: The average (so the mean) of all the SUVmean values.

Differentiating between active and non-active disease is important for treatment stratification as only active disease has a chance of reversibility with immunosuppressive treatment. HRCT scanning depicts anatomical changes and is therefore not accurate in the differentiation of active and non-active disease [4, 5, 8]. The ability of ^{18}F -FDG PET/CT to assess metabolic activity could add information on the reversibility of fibrosis and thus hypothetically be beneficial for treatment stratification and monitoring. Nevertheless, in our study we did not observe fibrotic tissue without increased ^{18}F -FDG uptake in dorso-basal lungs areas. A possible explanation may be that in all our patients with end-stage disease, the fibrosis may be metabolically active and not yet in remission. Moreover it may be hypothesized either that not only in our patients, but in all forms of fibrosis of SSc-ILD lungs—i.e. both early and end stage—there still is increased metabolic activity or that the ^{18}F -FDG tracer is not specific enough to distinguish between active and non-active fibrosis.

Previous studies have also indicated that ^{18}F -FDG PET/CT scanning is more sensitive than HRCT in the assessment of early-stage disease as normal-appearing HRCT lesions were associated with increased FDG-uptake [14, 15, 29]. In our study we did not observe normal lung tissue with increased ^{18}F -FDG uptake, which could be explained by the relatively long disease duration of our patients who are therefore not representative for early-stage disease.

Another explanation for the increased ^{18}F -FDG uptake in the areas of ground glass and reticulation and increased craniocaudal gradient of ^{18}F -FDG distribution may be that they are a result of a change in density, as it is known that the air, blood and tissue ratio influences the ^{18}F -FDG signal [33]. In our study we accounted for the physiological craniocaudal gradient through the calculation of B/A and M/A ratios. The significantly higher B/A ratios in SSc-ILD patients may be a result of increased cell metabolism or caused by a change in air/blood/tissue ratio other than the physiological craniocaudal gradient. Previous research showed that ILD lesions have a smaller air fraction and increased tissue fraction compared with controls [11]. It can be hypothesized that these changes in air and tissue fraction could lead to an increased ^{18}F -FDG uptake and higher B/A ratios in the absence of an absolute increase in metabolic activity.

In order to differentiate between these different hypotheses of increased ^{18}F -FDG uptake in ILD lesions it may be

helpful to use a dynamic scanning protocol that, in addition to our gradient correction, also corrects for local air and tissue fraction [32, 33]. Respiratory gated ^{18}F -FDG PET/CT scanning may also improve the accurate interpretation of ^{18}F -FDG uptake in dorso-basal lung areas [45]. Moreover, to distinguish between active and non-active ILD, the use of more specific PET tracers, targeting specific inflammatory cells or fibroblasts, may also improve the imaging of specific ILD-related histological changes in SSc.

This study was initiated as a preliminary investigation of the potential value for quantitative analyses of ^{18}F -FDG PET/CT scans in SSc-ILD patients and is therefore limited by the small number of patients and retrospective design. Also, with a mean disease duration of 5 years, the SSc-ILD patients in our study may not be representative for early-stage disease. Therefore, caution must be applied in extrapolating our results to SSc-ILD patients in general. Another limitation is the lack of follow-up ^{18}F -FDG PET/CT scans through which the value of this unique method for the prediction and monitoring of treatment response could have been evaluated. This is an important subject to address in future studies. It could have been of added value to correlate ^{18}F -FDG PET/CT results with PFT results. However, PFT results were only available in a few patients and did not add statistical value to this study and therefore were not included in our analysis.

In conclusion, in this study we showed that our newly developed method for semi-quantitative analysis of ^{18}F -FDG PET/CT scans was able to accurately distinguish ILD from non-ILD lung tissue. Semi-quantitative analysis of ILD in SSc may offer opportunities for patient stratification for immunosuppressive therapy and for monitoring of therapeutic efficacy. Further research is required on the optimization of ILD PET imaging in SSc.

Funding: No specific funding was received from any funding bodies in the public, commercial or not-for-profit sectors to carry out the work described in this manuscript.

Disclosure statement: The authors have declared no conflicts of interest.

Supplementary data

Supplementary data are available at *Rheumatology* online.

References

- 1 Steen VD, Medsger TA. Changes in causes of death in systemic sclerosis, 1972-2002. *Ann Rheum Dis* 2007;66:940-4.
- 2 Morales-Cardenas A, Perez-Madrid C, Arias L *et al.* Pulmonary involvement in systemic sclerosis. *Autoimmun Rev* 2016;15:1094-108.
- 3 Goh NS, Desai SR, Veeraraghavan S *et al.* Interstitial lung disease in systemic sclerosis: a simple staging system. *Am J Respir Crit Care Med* 2008;177:1248-54.
- 4 Denton CP, Khanna D. Systemic sclerosis. *Lancet* 2017;390:1685-99.
- 5 Antoniou KM, Margaritopoulos G, Economidou F, Siafakas NM. Pivotal clinical dilemmas in collagen vascular diseases associated with interstitial lung involvement. *Eur Respir J* 2009;33:882-96.
- 6 Kowal-Bielecka O, Fransen J, Avouac J *et al.* Update of EULAR recommendations for the treatment of systemic sclerosis. *Ann Rheum Dis* 2017;76:1327-39.
- 7 Schoenfeld SR, Castellino FV. Evaluation and management approaches for scleroderma lung disease. *Therapeutic Adv Respir Dis* 2017;11:327-40.
- 8 Wells AU. High-resolution computed tomography and scleroderma lung disease. *Rheumatology* 2008;47(Suppl 5):v59-61.
- 9 Le Gouellec N, Duhamel A, Perez T *et al.* Predictors of lung function test severity and outcome in systemic sclerosis-associated interstitial lung disease. *PLoS One* 2017;12:e0181692.
- 10 Behr J, Furst DE. Pulmonary function tests. *Rheumatology* 2008;47(Suppl 5):v65-7.
- 11 Chen DL, Schiebler ML, Goo JM, van Beek E. PET imaging approaches for inflammatory lung diseases: current concepts and future directions. *Eur J Radiol* 2017;86:371-6.
- 12 Jacquelin V, Mekinian A, Brillet PY *et al.* FDG-PET/CT in the prediction of pulmonary function improvement in nonspecific interstitial pneumonia. A pilot study. *Eur J Radiol* 2016;85:2200-5.
- 13 Justet A, Laurent-Bellue A, Thabut G *et al.* [¹⁸F]FDG PET/CT predicts progression-free survival in patients with idiopathic pulmonary fibrosis. *Respir Res* 2017;18:74.
- 14 Win T, Thomas BA, Lambrou T *et al.* Areas of normal pulmonary parenchyma on HRCT exhibit increased FDG PET signal in IPF patients. *Eur J Nucl Med Mol Imaging* 2014;41:337-42.
- 15 Nobashi T, Kubo T, Nakamoto Y *et al.* ¹⁸F-FDG uptake in less affected lung field provides prognostic stratification in patients with interstitial lung disease. *J Nucl Med* 2016;57:1899-904.
- 16 Umeda Y, Demura Y, Morikawa M *et al.* Prognostic value of dual-time-point ¹⁸F-FDG PET for idiopathic pulmonary fibrosis. *J Nucl Med* 2015;56:1869-75.
- 17 El-Chemaly S, Malide D, Yao J *et al.* Glucose transporter-1 distribution in fibrotic lung disease: association with [¹⁸F]-2-fluoro-2-deoxyglucose-PET scan uptake, inflammation, and neovascularization. *Chest* 2013;143:1685-91.
- 18 Wang ZG, Yu MM, Han Y *et al.* Correlation of Glut-1 and Glut-3 expression with F-18 FDG uptake in pulmonary inflammatory lesions. *Medicine (Baltimore)* 2016;95:e5462.
- 19 Bagnato G, Harari S. Cellular interactions in the pathogenesis of interstitial lung diseases. *Eur Respir Rev* 2015;24:102-14.
- 20 Todd NW, Scheraga RG, Galvin JR *et al.* Lymphocyte aggregates persist and accumulate in the lungs of patients with idiopathic pulmonary fibrosis. *J Inflamm Res* 2013;6:63-70.
- 21 Batra K, Butt Y, Gokaslan T *et al.* Pathology and radiology correlation of idiopathic interstitial pneumonias. *Hum Pathol* 2018;72:1-17.
- 22 Cohen C, Mekinian A, Uzunhan Y *et al.* ¹⁸F-fluorodeoxyglucose positron emission tomography/computer tomography as an objective tool for assessing disease activity in Sjogren's syndrome. *Autoimmun Rev* 2013;12:1109-14.
- 23 Uehara T, Takeno M, Hama M *et al.* Deep-inspiration breath-hold ¹⁸F-FDG-PET/CT is useful for assessment of connective tissue disease associated interstitial pneumonia. *Mod Rheumatol* 2016;26:121-7.
- 24 Nishiyama Y, Yamamoto Y, Dobashi H, Kameda T. Clinical value of ¹⁸F-fluorodeoxyglucose positron emission tomography in patients with connective tissue disease. *Jpn J Radiol* 2010;28:405-13.
- 25 Meissner HH, Soo Hoo GW, Khonsary SA *et al.* Idiopathic pulmonary fibrosis: evaluation with positron emission tomography. *Respiration* 2006;73:197-202.
- 26 Groves AM, Win T, Screation NJ *et al.* Idiopathic pulmonary fibrosis and diffuse parenchymal lung disease: implications from initial experience with ¹⁸F-FDG PET/CT. *J Nucl Med* 2009;50:538-45.
- 27 Lee EY, Wong CS, Fung SL, Yan PK, Ho JC. SUV as an adjunct in evaluating disease activity in idiopathic pulmonary fibrosis - a pilot study. *Nucl Med Commun* 2014;35:631-7.
- 28 Win T, Lambrou T, Hutton BF *et al.* ¹⁸F-Fluorodeoxyglucose positron emission tomography pulmonary imaging in idiopathic pulmonary fibrosis is reproducible: implications for future clinical trials. *Eur J Nucl Med Mol Imaging* 2012;39:521-8.
- 29 Bellando-Randone S, Tartarelli L, Cavigli E *et al.* ¹⁸F-fluorodeoxyglucose positron-emission tomography/CT and lung involvement in systemic sclerosis. *Ann Rheum Dis* 2019;78:577-8.
- 30 Travis WD, Costabel U, Hansell DM *et al.* An official American Thoracic Society/European Respiratory Society statement: update of the international multidisciplinary classification of the idiopathic interstitial pneumonias. *Am J Respir Crit Care Med* 2013;188:733-48.
- 31 Travis WD, Hunninghake G, King TE Jr *et al.* Idiopathic nonspecific interstitial pneumonia: report of an American Thoracic Society project. *Am J Respir Crit Care Med* 2008;177:1338-47.
- 32 Holman BF, Cuplov V, Millner L *et al.* Improved correction for the tissue fraction effect in lung PET/CT imaging. *Phys Med Biol* 2015;60:7387-402.
- 33 Chen DL, Cheriyan J, Chilvers ER *et al.* Quantification of lung PET images: challenges and opportunities. *J Nucl Med* 2017;58:201-7.

- 34 Galvin I, Drummond GB, Nirmalan M. Distribution of blood flow and ventilation in the lung: gravity is not the only factor. *Br J Anaesth* 2007;98:420–8.
- 35 Millar AB, Denison DM. Vertical gradients of lung density in healthy supine men. *Thorax* 1989;44:485–90.
- 36 van den Hoogen F, Khanna D, Fransen J *et al.* 2013 classification criteria for systemic sclerosis: an American College of Rheumatology/European League against Rheumatism collaborative initiative. *Arthritis Rheum* 2013;65:2737–47.
- 37 Hochberg MC. Updating the American College of Rheumatology revised criteria for the classification of systemic lupus erythematosus. *Arthritis Rheum* 1997;40:1725.
- 38 Shiboski CH, Shiboski SC, Seror R *et al.* 2016 American College of Rheumatology/European League Against Rheumatism Classification Criteria for Primary Sjogren's Syndrome: a consensus and data-driven methodology involving three international patient cohorts. *Arthritis Rheumatol (Hoboken)* 2017;69:35–45.
- 39 Boellaard R, Delgado-Bolton R, Oyen WJ *et al.* FDG PET/CT: EANM procedure guidelines for tumour imaging: version 2.0. *Eur J Nucl Med Mol Imaging* 2015;42:328–54.
- 40 Hansell DM, Bankier AA, MacMahon H *et al.* Fleischner society: glossary of terms for thoracic imaging. *Radiology* 2008;246:697–722.
- 41 Boktor RR, Walker G, Stacey R, Gledhill S, Pitman AG. Reference range for inpatient variability in blood-pool and liver SUV for ^{18}F -FDG PET. *J Nucl Med* 2013;54:677–82.
- 42 Meignan M, Gallamini A, Meignan M, Gallamini A, Haioun C. Report on the First International Workshop on Interim-PET-Scan in Lymphoma. *Leuk Lymphoma* 2009;50:1257–60.
- 43 Herzog EL, Mathur A, Tager AM *et al.* Review: interstitial lung disease associated with systemic sclerosis and idiopathic pulmonary fibrosis: how similar and distinct? *Arthritis Rheumatol (Hoboken)* 2014;66:1967–78.
- 44 Tanti JF, Gautier N, Cormont M *et al.* Potential involvement of the carboxy-terminus of the Glut 1 transporter in glucose transport. *Endocrinology* 1992;131:2319–24.
- 45 Froud R, McDermott G, Scarsbrook A. Respiratory-gated PET/CT for pulmonary lesion characterisation—promises and problems. *Br J Radiol* 2018;91:20170640.